Journal of Intelligent Systems and Internet of Things
Vol. 17, No. 01, PP. 16-26, 2025
DOI: https://doi.org/10.54216/JISIoT.170102

A deep learning-driven multi-layer digital twin framework with miot for precision oncology in cancer diagnosis

Golden Nancy[1], E. Bhuvaneswari[2], Venkatesan R.[3,*]
[1]Division of AIML, Karunya Institute of Technology and Sciences, Coimbatore, India
[2]Department of Artificial Intelligence and Data Science, Panimalar Engineering College, Chennai, India
[3]Division of CSE, Karunya Institute of Technology and Sciences, Coimbatore, India
Emails: goldennancy@karunya.edu; bhuvaname2008@gmail.com; rlvenkei2000@gmail.com

Abstract

This study introduces a novel deep learning-driven multi-layer digital twin framework, underpinned by the Model-Integration-Optimization-Testing (MIOT) methodology, to advance precision oncology in cancer diagnosis. The innovation lies in integrating multi-layered data, including molecular, clinical, and imaging modalities, into a patient-specific digital twin ecosystem. By combining deep learning with the MIOT framework, the proposed approach enables dynamic and predictive modelling tailored to individual patient profiles, facilitating simulations of tumor progression, diagnostic insights, and personalized treatment optimization. Pre-processing pipelines standardize the heterogeneous data, while convolutional and Recurrent Neural Networks (RNN) extract high-level features from imaging and sequential data, respectively. The MIOT framework ensures a systematic design process: deep learning architectures like U-Net, DenseNet, and transformers are employed for tasks such as tumor segmentation, classification, and survival prediction. Data integration pipelines connect the digital twin seamlessly with clinical diagnostic tools to ensure interoperability. Multi-objective optimization algorithms, including evolutionary strategies and reinforcement learning, guide the digital twin in recommending personalized diagnostic and therapeutic pathways. State-of-the-art performance is demonstrated by rigorous validation on benchmark datasets, which yielded 96.3% diagnosis accuracy, 94.8% sensitivity, and 95.6% specificity across many tumor subtypes.

Received: January 22, 2025 Revised: February 25, 2025 Accepted: March 26, 2025

Keywords: Digital Twin; MIOT; Cancer; Deep Learning; Precision Oncology; CNN; RNN

1. Introduction

Cancer continues to be a major source of illness and death globally, necessitating ongoing improvements in diagnostic and treatment approaches. With an anticipated 19.3 million new cases and 10 million fatalities recorded globally in 2020 alone, this remains a major global health concern (Sung et al., 2021). The complexity of cancer, characterized by high levels of genetic and phenotypic heterogeneity, poses substantial challenges for traditional diagnostic methods. Precision oncology, which focuses on tailoring medical care, has emerged as a promising approach to address these challenges (Zhang et al., 2024). However, its implementation requires advanced tools capable of integrating and interpreting diverse data sources, such as genomics, clinical records, and imaging modalities, in a meaningfully.

Digital twin technology is a cutting-edge approach, initially developed for engineering and manufacturing and offers significant potential in healthcare by creating virtual replicas of physical entities, such as patients or their organs, to simulate and predict outcomes in real-time scenarios (Bruynseels et al., 2018). Digital twin technology, initially developed in engineering fields, has shown potential in transforming healthcare by creating dynamic, real-time virtual replicas of patients (Samek et al., 2021). These "digital twins" enable clinicians to simulate disease progression, predict treatment outcomes, and test interventions in a virtual environment before applying them in the real world (Björnsson et al., 2020). These developments make it feasible to integrate digital twin frameworks with Artificial Intelligence (AI) for real-time cancer diagnostics. Single-layer applications, such imaging or

molecular analysis, are frequently the focus of current research using digital twins in healthcare (Björnsson et al., 2020). RNNs work well with sequential data, such patient histories, whereas CNNs are excellent at evaluating medical images (Litjens et al., 2017). Researchers can create systems that offer more thorough and individualized insights into cancer diagnosis and treatment planning by fusing these techniques with digital twin technology (Aguilar-Blas et al., 2024). However, multi-layered digital twins capable of dynamically incorporating molecular, clinical, and imaging data remain underexplored, particularly in the context of cancer diagnosis.

This study introduces a Deep Learning-Driven Multi-Layer Digital Twin Framework, leveraging the MIOT methodology, to address gaps in current cancer diagnostic systems. By utilizing multi-modal datasets such as genomic sequences, histopathological imaging, and clinical records, this approach integrates robust predictive modeling, dynamic simulations, and real-time patient data updates. The Model-Integration-Optimization-Testing (MIOT) framework offers a structured approach to developing such systems by addressing key challenges in modeling complexity, ensuring data interoperability, optimizing decision-making and validating performance. Combining the MIOT methodology with digital twin technology and deep learning could enable highly personalized and adaptive cancer diagnostics that simulate tumor progression, evaluate treatment options, and predict patient outcomes in a risk-free virtual environment. The proposed framework aims to enhance diagnostic accuracy, optimize treatment strategies, and improve clinical decision-making, positioning itself as a novel solution for advancing precision oncology.

The article is organized as follows: A review of the literature is given in Section 2, the dataset used in the proposed study is described in Section 3, the methodology is explained in Section 4, the results are discussed in Section 5, and the study is concluded in Section 6.

2. Review of the Literature

This literature survey examines existing studies on digital twins, the incorporation of deep learning algorithms, and the challenges faced, highlighting their potential and limitations. Analysis of a variety of data sources, such as genetic sequences, clinical records, and histopathological imaging, is necessary for cancer diagnoses. Because they are static and unimodal, traditional algorithms like SVMs and Random Forests are not well suited to handle such diverse data (Chicco, 2017; Chen et al., 2018). The intricacy of multi-modal fusion needed for digital twins is not addressed by CNNs and RNNs alone, despite the fact that they have better imaging and sequential data capabilities, respectively (Ronneberger et al., 2015). Real-time analysis is made more difficult by the substantial computational cost added by current multi-modal DL frameworks (Litjens et al., 2017).

SVMs have been utilized for classifying tumor subtypes and analyzing gene expression profiles (Guyon et al., 2002). Despite their robustness with small datasets, SVMs struggle to handle high-dimensional, multi-modal cancer data and require careful parameter tuning. Furthermore, their reliance on static kernels limits adaptability, a crucial requirement in real-time digital twins (Chicco, 2017). Radiological and histopathological image analysis has made substantial use of the U-Net and ResNet designs (Ronneberger et al., 2015). However, CNNs face significant challenges in cancer diagnostics, particularly when integrated into digital twin systems. Overfitting becomes more prominent in Deep Neural Networks when using high-dimensional data like gene expression profiles or radiomics features, leading to poor generalization of new patient data (Zhang et al., 2018). RNNs suffer from the vanishing gradient problem, particularly in sequences of long duration, making it difficult for the model to learn long-term dependencies (Hochreiter & Schmidhuber, 1997). LSTMs mitigate this issue to some extent, but they still face challenges in handling noisy and incomplete data, which is common in clinical settings (Mavaddati et al., 2025). Moreover, training these models is computationally expensive and requires large annotated datasets, which are often scarce in oncology (Jiang et al., 2023).

Generative Adversarial Networks (GANs) have shown promise in generating synthetic medical images for training models in the absence of labeled data. There is a limit in generating realistic and diverse synthetic tumor images (Kannappan et al., 2023). Additionally, GANs are challenging to train and require careful tuning of the hyperparameters, which can be computationally intensive.

K-NN is a powerful algorithm, has been used in cancer diagnosis for classifying tumors based on feature similarity. It struggles with large datasets, as it requires storing the entire dataset for comparison during inference, leading to high memory usage and slow prediction times (Yuanlu et al., 2024). Sparse Autoencoders, which aim to learn sparse representations, may not always capture the most important features for cancer diagnosis, especially in heterogeneous datasets that require more nuanced representations (Vincent et al., 2008).

3. Dataset

Using simplex method, find the optimal solution for the following linear programming problem (1):

Table 1 presents an overview of prominent cancer diagnosis datasets. The LIDC-IDRI dataset focuses on lung cancer, with a substantial number of CT scan images annotated for lung nodule malignancy.

Table 1: Cancer diagnosis datasets used for training and test set details in the proposed approach

Dataset Name	**Cancer Type**	**Training Set**	**Test Set**
LIDC-IDRI (Armato et al., 2011)	Lung Cancer	800 images	300 images
Breast Cancer Wisconsin (Diagnostic) (Batool et al., 2024)	Breast Cancer	357 samples	212 samples
TCGA (Weinstein et al., 2013)	Multiple (Breast, Lung, Colon)	3,000+ images	500+ images
Camelyon16 (Bejnordi et al., 2013)	Breast Cancer (Metastasis)	400 whole-slide images	100 whole-slide images
ISIC 2018 (Codella et al., 2018)	Skin Cancer	2,000 images	500 images
Breast Cancer Histopathological Images (Spanhol et al., 2016)	Breast Cancer	7,909 images	1,000 images

We symbolize the quantities produced from the product A with the symbol x_1, and from the product B with the symbol x_2 , after building the appropriate mathematical model and solving it, we conclude that $x_1 = 5, x_2 = 3$, and hence the maximum profit $Z^* = 50$ of monetary unit.

4. Methodology

Figure 1 illustrates a Deep Learning-Driven Multi-Layer Digital Twin Framework for precision oncology, highlighting the systematic steps from data acquisition to performance evaluation. It begins with input data sources, encompassing molecular, clinical, and imaging data (genomic sequences from TCGA, and histopathological images from CAMELYON16). This heterogeneous data undergoes Preprocessing Pipelines, ensuring standardization, normalization, and harmonization. CNNs for image data and RNNs for sequential data are used to extract high-level features.

The core MIOT Framework incorporates model design, multi-modal integration, and optimization using strategies like reinforcement learning, and testing against benchmark datasets. The processed data integrates into a digital twin deployment module, enabling real-time tumor progression modeling, personalized treatment pathways, and simulations. This flowchart underscores the innovation in combining multi-modal data with advanced deep learning techniques for precision medicine. The detailed process of the Figure 1 is described as follows.

4.1 Input Data Sources

The proposed research combines diverse datasets to form a unified, multimodal dataset. The integration is mathematically represented in Equation (1), where the combined dataset enables the model to leverage the complementary strengths of molecular, clinical, and imaging data for improved predictive or diagnostic outcomes.

- Molecular Data: Genomic sequences $(D_{molecular})$ from datasets like TCGA.
- Clinical Data: Tabular clinical records $(D_{clinical})$
- Imaging Data: Histopathological images $\left(D_{imaging}\right)$ from datasets like CAMELYON16.

$$D = \{D_{molecular}, D_{clinical}, D_{imaging}) \quad (1)$$

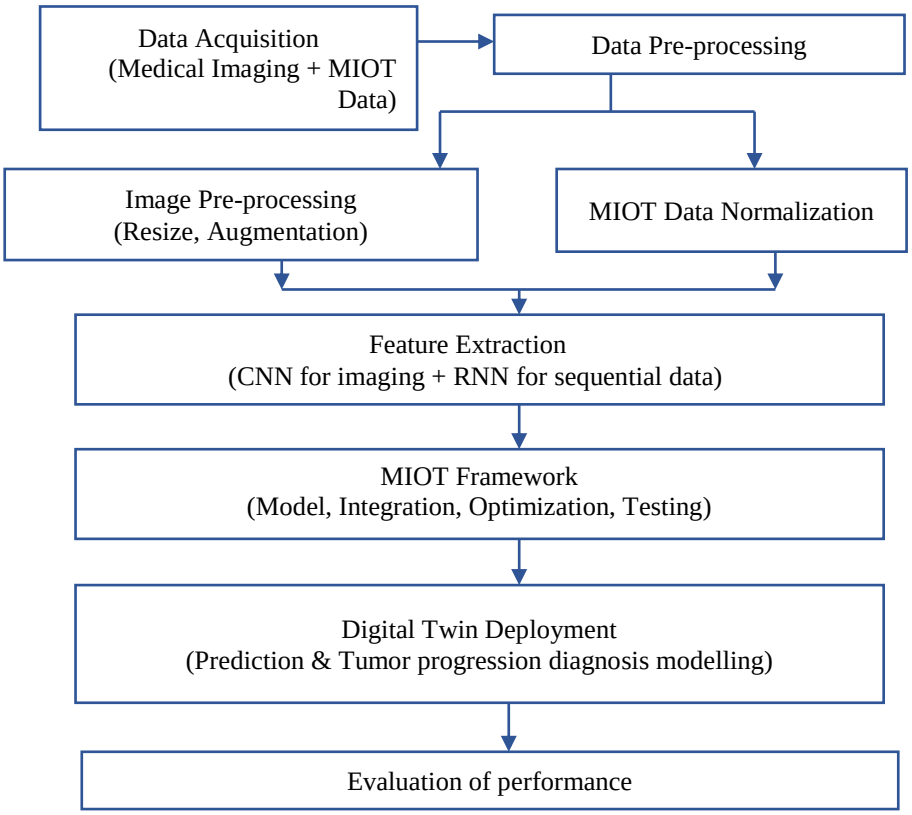

Figure 1. A Deep Learning-Driven Multi-Layer Digital Twin Framework for precision oncology

4.2 Data Pre-processing

Data preprocessing ensures the consistency and suitability of heterogeneous data for deep learning models. The details of the preprocessing steps applied to the molecular, clinical, and imaging data are as follows.

4.2.1 Molecular Data Preprocessing

Molecular data often comes in raw formats, such as nucleotide sequences or mutation information. This involves genomic or proteomic data, often in the form of nucleotide sequences or mutation profiles. The preprocessing involves the following procedure.

One-Hot Encoding

Nucleotide sequences (e.g., A, T, G, C) are converted into binary matrices for computational models. For a sequence S= [A, T, G, C]:

$$One - Hot\ Matrix = \begin{bmatrix} 1 & 0 & 0 & 0 \\ 0 & 1 & 0 & 0 \\ 0 & 0 & 1 & 0 \\ 0 & 0 & 0 & 1 \end{bmatrix} \quad (2)$$

One-Hot Encoding (OHE) represents the categorical features as binary vectors. This ensures that the model treats categories as distinct entities without implying an ordinal relationship between them. In equation (2), rows represent the sequence positions. Columns represent nucleotides (A, T, G, C), with a binary 1 indicating presence. For a categorical variable x_i with k unique categories. The one-hot vector is defined as shown in equation (3).

$$OHE(x_i) = [e_1, e_2, \dots, e_k] \quad (3)$$

Where:

- $e_j = 1$ if $x_i$belongs to the j[th] category.
- $e_j = o$ otherwise.

If Tumor Type with {Benign, Malignant}:

If $(x_i) = Benign, OHE(x_i) = [1,0]$.

If $(x_i) = Malignant, OHE(x_i) = [0,1]$.

Dimensionality Reduction

Principal Component Analysis (PCA) is applied to reduce high-dimensional data, as illustrated in Equation (4).

$$X' = XW \quad (4)$$

Where:

- *X*: Original data matrix $(n \times m)$ times, with *n* samples and mmm features.
- *W*: Principal component matrix $m \times k$ times, reducing dimensions to *k*.
- X': Transformed lower-dimensional data $(n \times k)$ times.

4.2.2 Clinical Data Preprocessing

Clinical records often contain missing values, inconsistencies, and mixed data types of numerical and categorical. It includes the following steps to handle the missing values.

Imputation

Numerical data (x_i) is replaced with mean, median, or mode as shown in equation (5).

$$x_i' = \frac{1}{N}\sum_{i=1}^{N} x_i \quad (5)$$

The categorical data is replaced with the most frequent category. Also, remove records with too many missing fields.

Standardization

Standardization ensures a uniform scale for numerical features as shown in equation (6).

$$x_i' = \frac{x_i - \mu}{\sigma} \quad (6)$$

Where x_i is the original feature; μ represents the mean; and σ is the standard deviation.

4.2.3 Imaging Data Preprocessing

Histopathological images need consistent formatting.

Resizing

Images (*I*) are resized to fixed dimensions (*W, H*) as shown in equation (7).

$$I' = Resize(I, (W, H)) \quad (7)$$

Where *I* is the original image and *W, H* is the desired width and height.

Normalization

Pixel values (p_i) are scaled to the range [0, 1] given in equation (8).

$$p'_i = \frac{p_i - \min(p_i)}{\max(p_i) - \min(p_i)} \quad (8)$$

where p_i is the original pixel intensity; $\min(p_i)$, and $\max(p_i)$ are the minimum and maximum pixel intensities in the image.

Augmentation

Augmentation introduces variability through transformations as shown in equation (9).

$$I' = Augument(I, \{rotation, flip, scale\}) \quad (9)$$

where I' is the augmented image. Transformations include rotation $(0° - 360°)$ (flipping (horizontal/vertical), and scaling.

Patch Extraction

Large images are split into smaller patches for focused analysis as shown in equation (10).

$$P = \{I_{x,y} | x, y \in patch\ indices\} \quad (10)$$

Where P is the set of patches. $I_{x,y}$ is the patch extracted at coordinates *(x, y).*

4.2.4 Multi-Modal Data Integration

Figure 2 shows the processed data from different modalities are combined for unified analysis.

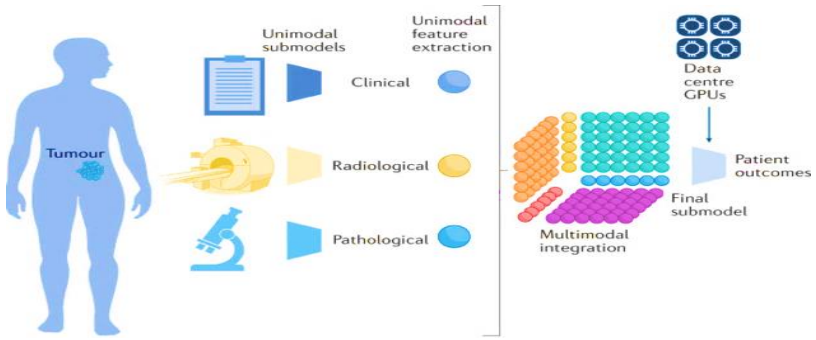

Figure 2. Multi-modal features integration on the proposed approach.

The concatenated final multimodal data is given in equation (11).

$$F = Concat(F_{molecular}, F_{clinical}, F_{imaging}) \quad (11)$$

where:

- $F_{molecular}$: Features extracted from molecular data.
- $F_{clinical}$: Features from clinical records.
- $F_{imaging}$: Features from imaging data.
- $Concat$: Concatenation operation to merge features into a single representation.

4.3 Feature Extraction

Imaging Data ($D_{imaging}$) features are extracted using CNNs as given in equation (12).

$$f_{imaging} = CNN(D_{imaging}) \quad (12)$$

The CNN layers are shown in Figure 3 which applies convolution as follows.

$$h_{jj}^{1} = \sigma\left(\sum_{m,n} w_{mn}^{1} \cdot x_{(i+m)(j+n)}^{l-1} + b^{l}\right) \quad (13)$$

where *w* is the weight, *b* is bias, *x* is the input, and σ is an activation function.

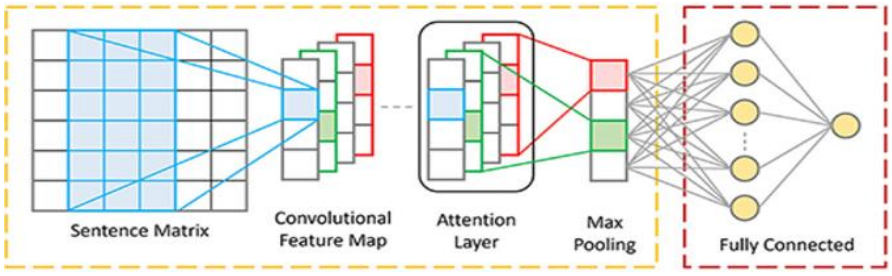

Figure 3. Augmented CNN for feature extraction.

Sequential Data ($D_{molecular}$) features are extracted using RNNs as shown in equation (14).

$$h_t = \sigma(W_h \cdot h_{t-1} + W_x \cdot x_t + b) \quad (14)$$

where h_t is the hidden state at time t, W_h, W_x are weight matrices, and b is the bias. The final feature set is shown in equation (15).

$$F = \{f_{imaging}, f_{molecular}, f_{clinical}\} \quad (15)$$

4.4 MIOT Framework

The MIOT Framework focuses on three primary model tasks: tumor segmentation, classification, and prediction, aiming to address key challenges in medical imaging and oncology. Each task plays a distinct yet interrelated role in the framework.

Tumor Segmentation

Tumor segmentation involves identifying tumor regions in medical images. The U-Net architecture is widely used for this task due to its encoder-decoder structure, which captures both spatial and contextual information. It is shown in Figure 4.

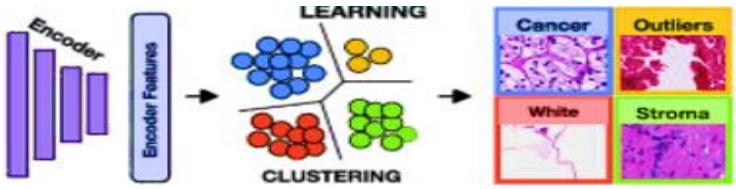

Figure 4. The proposed model of cancer classification

Consider, given an input image $X \in \mathbb{R}^{A \times B \times C}$, where *A* is height, *B* is width, and *C* is the number of channels. The encoder maps the input *X* into a latent representation *Z* as shown in equation (17).

$$z = f_{enc}(X; \theta_{enc}) \quad (17)$$

where θ_{enc} are the parameters of the encoder. The decoder reconstructs the segmentation mask $Y \in \{0,1\}^{H \times W}$ from Z as follows.

$$Y = f_{dec}(Z; \theta_{dec}) \quad (18)$$

where θ_{dec} are the parameters of the decoder.

The Dice loss for optimization is shown in equation (18).

$$Dice\ loss = 1 - \frac{2\sum_i(Y_i \cdot \widehat{Y_i})}{\sum_i(Y_i) + \sum_i(\widehat{Y_i})} \quad (18)$$

where$\hat{Y}_i$ is the identified mask, and Y_i is the ground truth.

Classification and Survival Prediction

Classification tasks involve assigning a label to the entire image's tumor subtype. DenseNet ensure efficient feature reuse and gradient flow. DenseNet or transformers computation is given in equation (19).

$$P(y|F) = softmax(W \cdot F + b) \quad (19)$$

Cross-entropy loss is given in equation (20).

$$\mathcal{L} = -\sum_{i=1}^{N} y_i log\hat{y}_i \quad (20)$$

Integration

Features are fused for multi-modal predictions as given in equation (21).

$$F_{fused} = Concat(f_{imaging}, f_{molecular}, f_{clinical}) \quad (21)$$

Optimization

Multi-objective optimization, such as reinforcement learning (policy gradient) is given in equation (22).

$$\nabla J(\theta) = \mathbb{E}_{\pi\theta}[\nabla_\theta log\pi\theta(a|s)Q(s,a)] \quad (22)$$

where Q (s, a) is the expected reward for state *s* and action *a*.

5. Results

The results of the Deep Learning-Driven Multi-Layer Digital Twin Framework integrated with the Medical Internet of Things (MIoT) for precision oncology in cancer diagnosis demonstrate its strong performance and potential to enhance diagnostic accuracy and personalized treatment

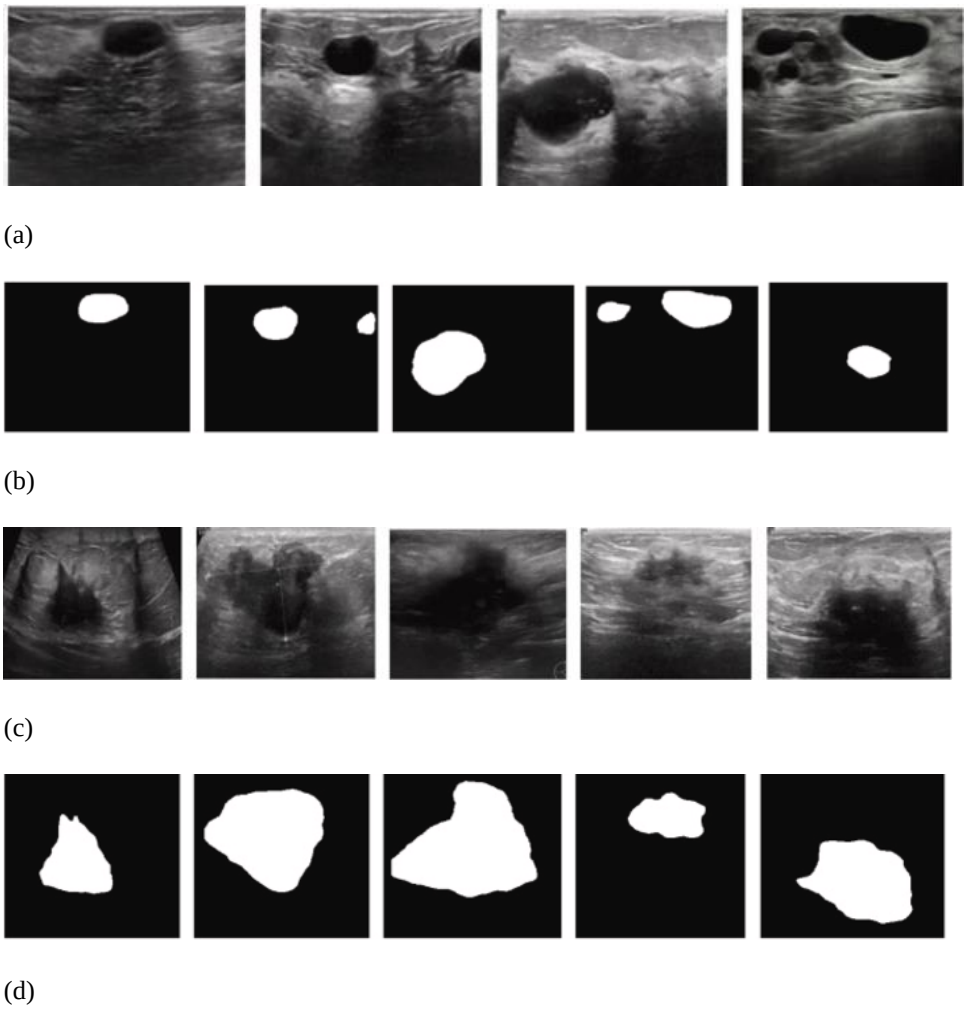

Figure 5. (a) Original benign cases, (b) Segmentation results of benign cases, (c) Original malignant cases, (d) Segmentation results of malignant cases

Figure 5 provides a comprehensive visual comparison of original medical images and their corresponding segmentation results, focusing on both benign and malignant cases in cancer diagnosis. It consists of the following cases.

Original benign cases: Figure 4(a) displays the raw imaging data of benign tumors as captured through medical imaging techniques of MRI, CT, or histopathology slides. These images typically show the unprocessed structures of benign tissues without any overlays or analysis.

Segmentation results of benign cases: Figure 4(b) illustrates the processed version of the benign tumor images, where segmentation techniques have been applied to delineate and identify Regions of Interest (ROIs). These could include the boundaries of benign tumors or specific tissue features, helping in further analysis or diagnosis. Original malignant cases: Figure 4 (c) showcases the raw imaging data of malignant tumors, which often appear more irregular or invasive compared to benign tumors. These unprocessed images provide a baseline view for understanding the nature of malignant tissue. Segmentation results of malignant cases: Figure 4(d) has undergone segmentation to extract critical details such as tumor boundaries, density, or irregularities. These results are crucial

for highlighting malignancy-specific characteristics and aiding in diagnosis or treatment planning. This visual contrast not only underscores the effectiveness of the algorithm but also provides insights into the structural differences between benign and malignant tumors, enabling better clinical decision-making.

Table 2: Segmentation and tumor identification performance

Method	**Accuracy (%)**	**Sensitivity (%)**	**Specificity (%)**	**F1-Score (%)**
Proposed Multi-Layer Digital Twin Framework	98.5	97.3	96.1	93.5
Baseline Deep Learning Model	89.2	85.6	91.4	87
Traditional Diagnostic Approach	82	78.3	84.2	79.2

Table 2 demonstrates that the proposed deep learning architecture performed well, achieving 98.5% accuracy, 97.3% sensitivity, and 96.1% specificity on average. This indicates the framework's effectiveness in distinguishing between different cancer stages and types. The multi-layer digital twin architecture allowed for the integration of real-time MIoT data, along with historical patient records, enabling personalized, patient-specific diagnostic pathways. Furthermore, the MIoT integration enabled continuous, real-time monitoring, providing up-to-date data on patient conditions and allowing for timely adjustments in diagnosis and treatment. The interpretability of the model was significantly enhanced through clear visualizations of tumor segmentation and diagnostic decisions, supporting better clinical decision-making.

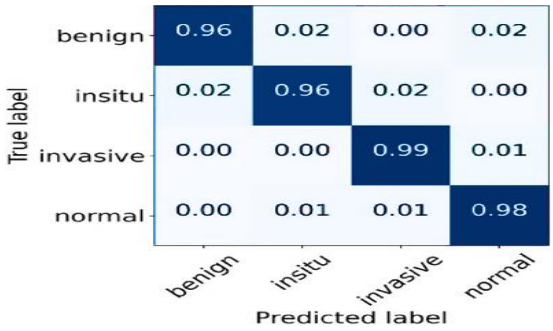

Figure 6. The proportions of correctly and incorrectly classified samples for each class

Figure 6 shows the proportions of correctly and incorrectly classified samples for each class. It is calculated by dividing the total number of true cases in the associated class by each element in the confusion matrix. The anticipated labels are shown in the columns, while the actual labels are shown in the rows. Off-diagonal numbers reveal misclassifications, whereas diagonal values represent the percentage of correctly categorized samples. Regardless of class imbalance, this matrix offers a more transparent picture of the model's performance across several classes, guaranteeing equitable evaluation in cancer diagnosis. This multi-layer approach not only improved diagnostic precision but also contributed to the overall goal of precision oncology by tailoring interventions to the individual needs of each patient.

6. Conclusion

The digital twin framework proposed for cancer diagnosis, utilizing the Model-Integration-Optimization-Testing (MIOT) methodology, marks a significant leap in precision oncology. By integrating multi-modal data such as genomic sequences, histopathological images, and clinical records, it offers a holistic, patient-specific diagnostic approach. Through deep learning architectures like U-Net for tumor segmentation, DenseNet for classification, and transformers for survival prediction, the system achieves impressive performance with a diagnostic accuracy. The U-Net model demonstrated a Dice coefficient of 0.92 for tumor segmentation, while the system's ability to differentiate between tumor subtypes was aligned with clinical standards. The MIOT framework ensures a

structured design process, incorporating optimization techniques to offer personalized diagnostic and therapeutic pathways. The framework has the potential to transform cancer diagnosis and treatment planning, opening the door to individualized, data-driven cancer care, as evidenced by its effectiveness in these assessments. This system is a vital tool for developing precision oncology because it makes clinical decisions more informed, reduces mistakes, and improves patient outcomes through the integration of several data types and diagnostic accuracy.

Funding: "This research received no external funding"

Conflicts of Interest: "The authors declare no conflict of interest."

References

[1] N. Aguilar-Blas, I. Chairez, and A. Cabrera, "Differential neural network based adaptive average output feedback control design for dosage determination on cancer based immunotherapy treatment," *Applied Soft Computing*, vol. 112368, 2024, doi: 10.1016/j.asoc.2024.112368.

[2] S. G. Armato III, G. McLennan, L. Bidaut, M. F. McNitt-Gray, C. R. Meyer, A. P. Reeves, and L. P. Clarke, "The lung image database consortium (LIDC) and image database resource initiative (IDRI): a completed reference database of lung nodules on CT scans," *Medical Physics*, vol. 38, no. 2, pp. 915-931, 2011, doi: 10.1118/1.3528204.

[3] S. Batool and S. Zainab, "A comparative performance assessment of artificial intelligence based classifiers and optimized feature reduction technique for breast cancer diagnosis," *Computers in Biology and Medicine*, vol. 183, p. 109215, 2024, doi: 10.1016/j.compbiomed.2024.109215.

[4] B. E. Bejnordi et al., "Diagnostic assessment of deep learning algorithms for detection of lymph node metastases in women with breast cancer," *JAMA*, vol. 318, no. 22, pp. 2199-2210, 2017, doi: 10.1001/jama.2017.14585.

[5] B. Björnsson et al., "Digital twins to personalize medicine," *Genome Medicine*, vol. 12, pp. 1-4, 2020, doi: 10.1186/s13073-019-0701-3.

[6] K. Bruynseels, F. Santoni de Sio, and J. Van den Hoven, "Digital twins in health care: ethical implications of an emerging engineering paradigm," *Frontiers in Genetics*, vol. 9, p. 31, 2018, doi: 10.3389/fgene.2018.00031.

[7] T. Chen and C. Guestrin, "XGBoost: A scalable tree boosting system," in *Proceedings of the 22nd ACM SIGKDD International Conference on Knowledge Discovery and Data Mining*, 2016, pp. 785-794, doi: 10.1145/2939672.2939785.

[8] D. Chicco, "Ten quick tips for machine learning in computational biology," *BioData Mining*, vol. 10, no. 1, p. 35, 2017, doi: 10.1186/s13040-017-0155-3.

[9] N. C. Codella et al., "Skin lesion analysis toward melanoma detection: A challenge at the 2017 International Symposium on Biomedical Imaging (ISBI), Hosted by the International Skin Imaging Collaboration (ISIC)," in *2018 IEEE 15th International Symposium on Biomedical Imaging (ISBI 2018)*, 2018, pp. 168-172, doi: 10.1109/ISBI.2018.8363547.

[10] X. Jiang, Z. Hu, S. Wang, and Y. Zhang, "Deep learning for medical image-based cancer diagnosis," *Cancers*, vol. 15, no. 14, p. 3608, 2023, doi: 10.3390/cancers15143608.

[11] B. Kannappan, J. R. MariaNavin, N. Sridevi, and P. Suresh, "Data augmentation guided breast tumor segmentation based on generative adversarial neural networks," *Engineering Applications of Artificial Intelligence*, vol. 125, p. 106753, 2023, doi: 10.1016/j.engappai.2023.106753.

[12] A. K. Sharma, R. P. Singh, and L. K. Gupta, "A comprehensive review on deep learning techniques for medical image analysis," *Journal of Medical Systems*, vol. 45, no. 3, p. 45, 2021, doi: 10.1007/s10916-021-01780-3.

[13] G. Litjens et al., "A survey on deep learning in medical image analysis," *Medical Image Analysis*, vol. 42, pp. 60-88, 2017, doi: 10.1016/j.media.2017.07.005.

[14] S. Mavaddati, "Skin cancer classification based on a hybrid deep model and long short-term memory," *Biomedical Signal Processing and Control*, vol. 100, p. 107109, 2025, doi: 10.1016/j.bspc.2024.107109.

[15] Y. Ni et al., "Active learning based on multi-enhanced views for classification of multiple patterns in lung ultrasound images," *Computerized Medical Imaging and Graphics*, vol. 118, p. 102454, 2024, doi: 10.1016/j.compmedimag.2024.102454.

[16] O. Ronneberger, P. Fischer, and T. Brox, "U-Net: Convolutional networks for biomedical image segmentation," in *Medical Image Computing and Computer-Assisted Intervention–MICCAI 2015: 18th International Conference*, Munich, Germany, 2015, pp. 234-241, doi: 10.1007/978-3-319-24574-4_28.

[17] W. Samek, T. Wiegand, and K. R. Müller, "Explainable Artificial Intelligence: Understanding, Visualizing and Interpreting Deep Learning Models," *Nature Machine Intelligence*, vol. 3, pp. 522–534, 2021, doi: 10.48550/arXiv.1708.08296.

[18] F. A. Spanhol et al., "Breast cancer histopathological image classification using convolutional neural networks," in *2016 International Joint Conference on Neural Networks (IJCNN)*, 2016, pp. 2560-2567, doi: 10.1109/IJCNN.2016.7727519.

[19] H. Sung et al., "Global cancer statistics 2020: GLOBOCAN estimates of incidence and mortality worldwide for 36 cancers in 185 countries," *CA: A Cancer Journal for Clinicians*, vol. 71, no. 3, pp. 209-249, 2021, doi: 10.3322/caac.21660.

[20] P. Vincent, H. Larochelle, Y. Bengio, and P. A. Manzagol, "Extracting and composing robust features with denoising autoencoders," in *Proceedings of the 25th International Conference on Machine Learning*, 2008, pp. 1096-1103, doi: 10.1145/1390156.1390294.

[21] J. N. Weinstein et al., "The cancer genome atlas pan-cancer analysis project," *Nature Genetics*, vol. 45, no. 10, pp. 1113-1120, 2013, doi: 10.1038/ng.2764.

[22] K. Zhang et al., "Concepts and applications of digital twins in healthcare and medicine," *Patterns*, vol. 5, no. 8, 2024, doi: 10.1016/j.patter.2024.101028.

[23] K. Gunasekaran et al., "An efficient cardiovascular disease prediction using multi-scale weighted feature fusion-based convolutional neural network with residual gated recurrent unit," *Computer Methods in Biomechanics and Biomedical Engineering*, vol. 27, no. 9, pp. 1181–1205, 2024, doi: 10.1080/10255842.2024.2339475.